

Organic & Biomolecular Chemistry

Accepted Manuscript



This is an *Accepted Manuscript*, which has been through the Royal Society of Chemistry peer review process and has been accepted for publication.

Accepted Manuscripts are published online shortly after acceptance, before technical editing, formatting and proof reading. Using this free service, authors can make their results available to the community, in citable form, before we publish the edited article. We will replace this *Accepted Manuscript* with the edited and formatted *Advance Article* as soon as it is available.

You can find more information about *Accepted Manuscripts* in the [Information for Authors](#).

Please note that technical editing may introduce minor changes to the text and/or graphics, which may alter content. The journal's standard [Terms & Conditions](#) and the [Ethical guidelines](#) still apply. In no event shall the Royal Society of Chemistry be held responsible for any errors or omissions in this *Accepted Manuscript* or any consequences arising from the use of any information it contains.



Journal Name

ARTICLE

Synthesis of 8-aza-3,7-dideaza-2'-deoxyadenosines possessing a new adenosine skeleton as an environmentally sensitive fluorescent nucleoside for monitoring DNA minor groove

Received 00th January 20xx,
Accepted 00th January 20xx

DOI: 10.1039/x0xx00000x

www.rsc.org/

Azusa Suzuki, Mio Saito, Ryuzi Katoh and Yoshio Saito*

8-Aza-3,7-dideaza-2'-deoxyadenosine **1** and its C3-naphthylethynylated derivative $^{3nz}\mathbf{A}$ (**2**) comprising a 8-aza-3,7-dideazapurine (pyrazolo[4,3-c]pyridine) skeleton were synthesized for the first time. In particular, nucleoside $^{3nz}\mathbf{A}$ (**2**) exhibited environmentally sensitive intramolecular charge transfer (ICT) emission because of electron transition in the coplanar conformer formed by nucleobase and naphthalene moieties. Its incorporation into oligodeoxynucleotide (ODN) probes enable a clear identification of a perfectly matched thymine (T) in the complementary strand by a distinct change in emission wavelength. In addition, the fluorescence emission of the duplexes containing a cytosine/guanine (C/G) base pair flanking $^{3nz}\mathbf{A}$ (**2**) was strongly quenched by guanine only when the opposite base of the modified nucleoside was mismatched, enhancing its base identification ability. Thus, ODN probes containing $^{3nz}\mathbf{A}$ (**2**) acted as effective reporter probes for homogeneous single nucleotide polymorphism (SNP) typing.

Introduction

Fluorescent molecules play an important role as research tools in diverse fields such as chemical biology and medicinal chemistry.¹ In particular, environmentally sensitive fluorescent (ESF) molecules that elucidate microenvironmental fluctuations such as polarity and viscosity variations through changes in emission wavelength and intensity may act as powerful tools for investigations of the local structure, dynamics, and functions of biomolecules.² Numerous ESF molecules have been developed and incorporated into various biopolymers, such as proteins, lipids, and nucleic acids, in which they served as reporter molecules. ESF amino acid analogs have been designed for *in vitro* and *in vivo* protein structure and function studies.³ Various base-modified fluorescent nucleosides have also been reported.⁴ Among them, several C5-substituted fluorescent pyrimidine nucleosides exhibited environmentally sensitive properties.^{4f-i} Srivatsan and co-workers developed solvatochromic benzofurano-conjugated uridine derivatives that specifically signal the presence of a DNA abasic site in an RNA/DNA heteroduplex.^{4f} Tor *et al.* have detected an abasic site in DNA duplexes by fluorescence intensity change using the viscosity- and polarity-sensitive furan-modified deoxyuridine.^{4h} In addition, solvatochromic pyrimidine nucleosides containing GFP-like fluorophores have been

generated to study DNA-protein interactions.⁴ⁱ However, to date, no fluorescent nucleoside capable of discriminating structural changes in oligonucleotides, such as single-base mismatches in DNA duplexes, by a distinct variation in the emission wavelength when incorporated into oligonucleotide probes has been synthesized.

Our continuous efforts at developing useful base-modified ESF nucleosides sensing microenvironmental changes⁵ have recently led to several solvatochromic purine nucleosides such as C7-substituted 8-aza-7-deazapurine and C3-substituted 3-deazaadenine derivatives comprising an electron donor-acceptor system within a molecule.⁶ These charge-transfer fluorescent nucleosides acted as excellent ESF purine nucleosides, forming stable Watson-Crick base pairs, and displaying changes in the emission wavelength on hybridization with target DNA/RNA sequences. DNA probes containing C3-naphthylethynylated 3-deaza-2'-deoxyadenosine $^{3nz}\mathbf{A}$ clearly discriminated a perfectly matched thymine in the complementary strand by indicating a change in the emission wavelength resulting from environmental variation in the DNA minor groove (Fig. 1).^{6c} However, ESF nucleosides exhibiting high sensitivity and strong fluorescence emissions associated with larger Stokes shifts remain in great demand, prompting the design of novel $^{3nz}\mathbf{A}$ derivatives displaying enhanced response to microenvironmental changes.

To tune the electron donating/accepting ability of the $^{3nz}\mathbf{A}$ nucleobase according to the design concept of these charge-transfer molecules, this study focuses on 8-aza-3,7-dideaza-2'-deoxyadenosine **1**, a novel nucleoside comprising a 8-aza-3,7-dideazapurine (pyrazolo[4,3-c]pyridine) skeleton. Although this skeleton structurally closely resembles 3-deazaadenine (4-aminoimidazo[4,5-c]pyridine) present in $^{3nz}\mathbf{A}$, its electron donating/accepting ability should differ, as suggested by redox potential estimates. In addition, except $^{3nz}\mathbf{A}$, no ESF nucleoside has

Department of Chemical Biology and Applied Chemistry, College of Engineering, Nihon University, Koriyama, Fukushima 963-8642, Japan. Fax: +81 (0)24 956 8924; Tel: +81 (0)24 956 8809; E-mail: saito@chem.ce.nihon-u.ac.jp

† Electronic Supplementary Information (ESI) available: ¹H- and ¹³C-NMR spectra of newly synthesized compounds, optimized structure of N^β-methylated $^{3nz}\mathbf{A}$, absorption and excitation spectra of $^{3nz}\mathbf{A}$ in various solvents, and HPLC profiles, MALDI-TOF-mass, CD, absorption and excitation spectra of $^{3nz}\mathbf{A}$ -containing ODNs]. See DOI: 10.1039/x0xx00000x

shown the ability to probe the DNA minor groove microenvironment. Therefore, the C3-naphthylethynylated 8-aza-3,7-dideaza-2'-deoxyadenosine derivative ^{3n7z}A (**2**) was designed as a novel ESF purine nucleoside. This study reports the synthesis of this derivative and its 8-aza-3,7-dideaza-2'-deoxyadenosine precursor. The ESF nucleoside ^{3n7z}A (**2**) was incorporated into oligodeoxynucleotides (ODNs), and its photophysical properties were evaluated along with its base discrimination ability.

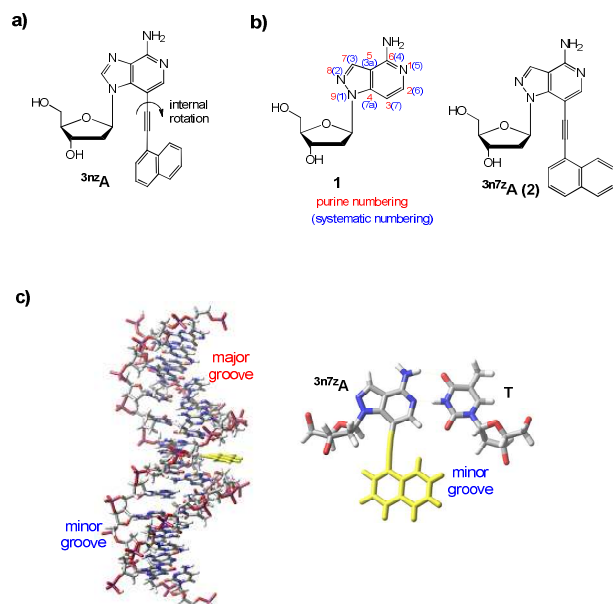


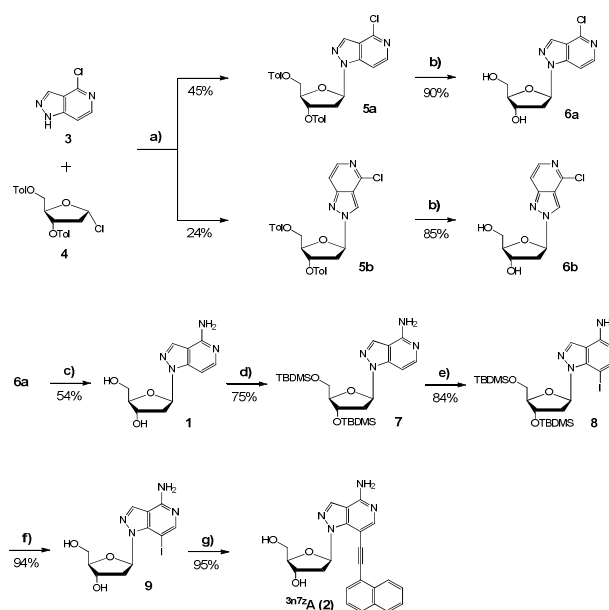
Figure 1. Structures of 3-deazapurine nucleosides (with numbering system). Purine numbering is used throughout this manuscript for consistency. (a) Previously reported C3-naphthylethynylated 3-deaza-2'-deoxyadenosine ^{3n7z}A . (b) Newly designed 8-aza-3,7-dideaza-2'-deoxyadenosine **1** (left) and its C3-naphthylethynylated derivative ^{3n7z}A (**2**) (right). (c) Structural model showing a $^{3n7z}A/T$ base pair in a DNA duplex. The model was optimized using the AMBER* force field in water by Macromodel (ver. 9.0).

Results and discussion

The synthetic route followed to generate 8-aza-3,7-dideaza-2'-deoxyadenosine **1** and its C3-naphthylethynylated derivative ^{3n7z}A (**2**) is shown in Scheme 1. 4-Chloro-1*H*-pyrazolo[4,3-*c*]pyridine **3** was prepared from 3-formyl-2,4-dichloropyridine and hydrazine monohydrate and glycosylated in the presence of α -D-2-deoxyribofuranosyl halide **4** to give nucleosides **5a** and **5b** in 69% yield with a N^9/N^8 -glycoside ratio of 65:35 (purine numbering). The regioisomers were separated by silica gel column chromatography and deprotected with NaOMe in methanol to provide **6a** and **6b**, which were characterized by NMR spectroscopy. The glycosylation position in these isomers was derived from their ^{13}C NMR spectra (Table 1). The C-7 atom displayed an upfield shift in isomer **6b** compared to **6a**, which exhibited chemical shifts similar to free nucleobase **3**, suggesting that **6a** was the desired isomer.⁷ Glycosylation position and anomeric configuration in both compounds were assessed by nuclear Overhauser effect (NOE) spectroscopy. Correlations observed for H-C(3) and H-C(4') on the saturation of H-C(1') indicated that **6a** was the N^9 -isomer with a β -D configuration. On the other hand, NOEs were detected at H-C(7) and H-C(4') on the irradiation of H-C(1') in **6b**, suggesting that this

compound was the N^8 -isomer with a β -D configuration (Fig. 2).⁸ Isomer **6a** was consequently converted into target nucleoside **1**. Because 8-aza-6-chloro-3,7-dideazapurine nucleoside **6a** presented a low reactivity toward nucleophiles such as ammonia in S_NAr reactions, the amination was achieved via an alternative two-step reaction. Specifically, the displacement of the 6-Cl substituent using hydrazine and subsequent Raney-nickel reduction of the hydrazino intermediate provided 8-aza-3,7-dideaza-2'-deoxyadenosine **1**.

Nucleoside **1** was further reacted to produce C3-naphthylethynylated derivative ^{3n7z}A (**2**). The protection of the 5'- and 3'-hydroxyl groups with *tert*-butyldimethylsilyl chloride (TBDMSCl) gave **7**, which generated 3',5'-diprotected **8** in the presence of *N*-iodosuccinimide in DMF. Tetra-*N*-butylammonium fluoride (TBAF) treatment of **8** provided 8-aza-3,7-dideaza-3-iodo-2'-deoxyadenosine **9**, which underwent Pd(PPh₃)₄ catalyzed cross-coupling with 1-ethynynaphthalene to give C3-naphthylethynylated 8-aza-3,7-dideaza-2'-deoxyadenosine ^{3n7z}A (**2**).⁹



Scheme 1. Reagents and conditions: a) NaH, acetonitrile, 50 °C, 1 h, then rt, 30 min; b) 0.5 M NaOMe/MeOH, rt, 30 min; c) hydrazine, 90 °C, 2 h, then Raney-Nickel, EtOH, reflux, 2 h; d) TBDMSCl, imidazole, DMF, rt, overnight; e) *N*-iodosuccinimide, DMF, rt, overnight; f) TBAF, THF, rt, 1 h; g) 1-ethynynaphthalene, Pd(PPh₃)₄, CuI, Et₃N, DMF, 60 °C, 1 h.

Table 1. ^{13}C -NMR chemical shifts (δ) of 8-aza-3,7-dideazapurine 2'-deoxyribonucleosides in DMSO-*d*₆.

	C(2) ^a	C(3) ^a	C(4) ^a	C(5) ^a	C(6) ^a	C(7) ^a	C(1')	C(2')	C(3')	C(4')	C(5')
3	142.9	105.6	144.0	118.8	143.3	133.0					
5a	143.7	105.4	144.4	119.8	143.5	134.2	86.4	35.7	74.7	81.7	63.8
5b	141.5	111.4	150.4	118.2	145.0	126.3	90.7	37.3	74.6	82.7	63.8
6a	143.6	105.5	144.0 ^b	119.7	143.4 ^b	133.7	86.4	38.4	70.8	87.9	62.1
6b	141.3	111.4	150.1	118.1	144.8	124.9	91.1	40.7	70.0	88.6	61.4
1	144.0	94.6	144.4	108.1	154.0	133.8	85.6	38.3	71.0	87.5	62.4
9	152.0	55.4	143.0	110.6	154.0	133.9	84.2	38.1	71.1	87.6	62.4

^a Purine numbering

^b Assigned by HMBC spectroscopy

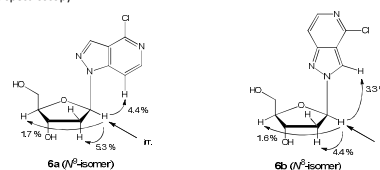


Figure 2. NOE correlations in nucleosides **6a** and **6b**.

Initially, the fluorescence spectra of $^{3n7z}\mathbf{A}$ (**2**) in solvents of various polarities and viscosities were obtained. Excitation at 351 nm in 1,4-dioxane resulted in a strong broad emission band at 398 nm ($\phi_F = 0.68$, Fig. 3 and Table 2). In contrast, the fluorescence emission in more polar solvents such as DMSO was weak and shifted toward a longer wavelength (445 nm, $\phi_F = 0.43$). The Stokes shift ($\Delta\nu$) of $^{3n7z}\mathbf{A}$ (**2**) observed in different solvents was plotted against the dielectric constant (ϵ) of each solvent. The shift significantly depended on solvent polarity and increased proportionally with increasing dielectric constant (Fig. 3b). Therefore, the broad emission band of $^{3n7z}\mathbf{A}$ (**2**) exhibited a reasonably large solvatochromicity ($\Delta\lambda = 47$ nm), which was assigned to the emission from intramolecular charge-transfer (ICT) state, and significantly shifted to longer wavelengths in highly polar solvents.

Next, the dependence of the fluorescence wavelength on solvent viscosity was examined (Fig. 3c-d). When the structurally similar compound $^{3nz}\mathbf{A}$ was dissolved in a high-viscosity solvent such as glycerol ($\eta = 1420$ mPa s, 20 °C), sharp vibronic emission bands were observed at largely blue-shifted wavelengths as previously reported (Fig. 3d).^{6c} The high viscosity disturbed the rotation of the naphthalene moiety in $^{3nz}\mathbf{A}$, and the more stable twisted ground-state conformation was preferred. As a result, the emission of the naphthalene moiety predominated from the locally excited (LE) state in the blue-shifted region.^{6c} In contrast, $^{3n7z}\mathbf{A}$ (**2**) did not exhibit any vibronic LE emission from the electronic transition of the twisted conformer (Fig. 3c). As judged from the fluorescence dependency on solvent viscosity, $^{3n7z}\mathbf{A}$ (**2**) probably adopted a coplanar ground state conformation and only displayed an unstructured ICT emission from the electron transition of this conformer. No significant change was observed in the UV-visible absorption spectra when solvent viscosity increased for $^{3n7z}\mathbf{A}$ (**2**) (Fig. 3c-d). In contrast, $^{3nz}\mathbf{A}$ exhibited largely blue-shifted absorption bands. In addition to supporting this hypothesis, these results indicate that $^{3n7z}\mathbf{A}$ (**2**) adopted very similar ground state conformations in glycerol and low-viscosity 1,4-dioxane ($\eta = 1.44$ mPa s, 20 °C). DFT calculations have also suggested that 8-aza-3,7-dideazaadenine and the naphthalene ring were coplanar in the ground-state structure (supplementary data, Fig. S1). The difference of the structure between $^{3n7z}\mathbf{A}$ (**2**) and $^{3nz}\mathbf{A}$ is probably due to the balance of the electron donating/accepting ability between nucleobase and naphthalene rings. In fact, 8-aza-3,7-dideaza-2'-deoxyadenosine **1** ($E_{ox} = 1.17$ V vs. the saturated calomel electrode (SCE)) showed a different electron donating ability from 3-deaza-2'-deoxyadenosine ($E_{ox} = 1.06$ V vs. SCE).

Table 2. Photophysical properties of $^{3n7z}\mathbf{A}$ (**2**) with solvent properties

Solvents	ϵ^a	η^b	λ_{max}^{em} (nm)	ν_{ss} (cm ⁻¹) ^c	ϕ_F^d
1,4-dioxane	2.21	1.44	398	3364	0.68
ethyl acetate	6.05	0.45	404	3819	0.45
THF	7.58	0.58	408	3899	0.49
DMF	36.7	0.92	437	5286	0.33
DMSO	46.4	1.99	445	5461	0.43
acetonitrile	35.9	0.34	425	5124	0.23
2-propanol	19.9	2.04	412	4547	0.17
ethanol	24.6	1.20	415	4722	0.13
methanol	32.7	0.59	422	5373	0.06
ethylene glycol	37.7	19.9	425	5124	0.27
glycerol	42.5	1412	424	4987	0.58

^a Dielectric constant

^b Viscosity (mPa s) [at 20 °C]

^c Stokes shift

^d Fluorescence quantum yields were calculated according to Ref.10

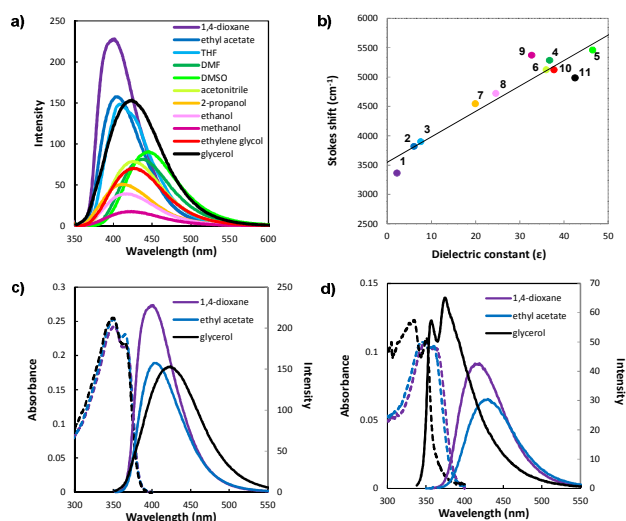
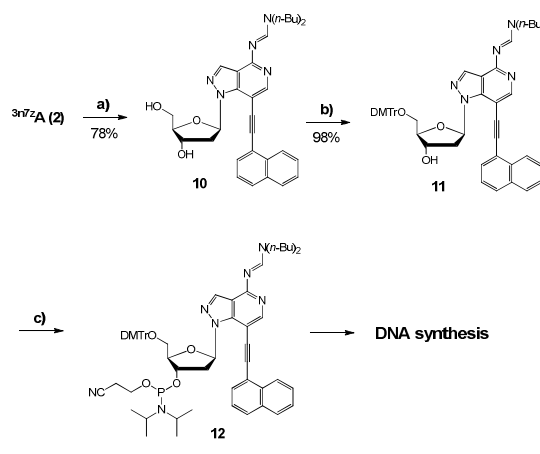


Figure 3. (a) Fluorescence spectra of $^{3n7z}\mathbf{A}$ (**2**) in various solvents. (b) Stokes shifts of $^{3n7z}\mathbf{A}$ (**2**) as a function of solvent: 1, 1,4-dioxane; 2, ethyl acetate; 3, THF; 4, DMF; 5, DMSO; 6, acetonitrile; 7, 2-propanol; 8, ethanol; 9, methanol; 10, ethylene glycol; 11, glycerol. Absorption (dotted line) and fluorescence spectra (solid line) of (c) $^{3n7z}\mathbf{A}$ (**2**) and (d) $^{3nz}\mathbf{A}$ in 1,4-dioxane, ethyl acetate, and glycerol. All measurements were performed at a concentration of 10 μM .

The solvatochromicity of nucleoside $^{3n7z}\mathbf{A}$ (**2**) is expected to be valuable for monitoring DNA microenvironmental changes originating from structural modifications, such as duplex formation and mismatches. Therefore, the thermal stability and photophysical properties of DNA oligomers containing this newly developed ESF nucleoside were investigated by incorporating $^{3n7z}\mathbf{A}$ (**2**) into ODNs *via* automated DNA synthesis. The synthesis of the corresponding phosphoramidite is shown in Scheme 2. The protection of the amino group using *N,N*-di-*n*-butylformamide dimethylacetal in $^{3n7z}\mathbf{A}$ (**2**) gave compound **10**, which reacted with DMTrCl in dry pyridine to produce **11**. Nucleoside **11** was subsequently converted into phosphoramidite **12**, which was used for ODN synthesis in an automated DNA/RNA synthesizer without further purification. Two 13-mer fluorescent ODN probes containing ESF nucleoside $^{3n7z}\mathbf{A}$ (**2**) in AT-rich (ODN1($^{3n7z}\mathbf{A}$)) and GC-rich sites (ODN2($^{3n7z}\mathbf{A}$)) were initially synthesized (Table 3).



Scheme 2. Reagents and conditions: a) *N,N*-di-*n*-butylformamide dimethyl acetal, DMF, 80 °C, 2 h; b) DMTrCl, pyridine, rt, 2 h; c) 2-cyanoethyl diisopropylchlorophosphoramidite, Et₃N, acetonitrile, rt, 30 min.

Table 3. Oligonucleotides used in this study

ODNs	Sequences	
ODN1(X)	5'-d(CGCAATXTAACGC)-3'	X = ^{3n7z} A or A
ODN2(X)	5'-d(CGCAACXCAACGC)-3'	X = ^{3n7z} A or A
ODN3(X)	5'-d(CGCAATXCAACGC)-3'	X = ^{3n7z} A or A
ODN4(X)	5'-d(CGCAACXTAACGC)-3'	X = ^{3n7z} A or A
ODN5(X)	5'-d(CGCACTXTCACGC)-3'	X = ^{3n7z} A or A
ODN6(X)	5'-d(CGCAGTXTGACGC)-3'	X = ^{3n7z} A or A
cODN1(N)	5'-d(GCGTTANATTGCG)-3'	N = A, G, C, or T
cODN2(N)	5'-d(GCGTTGNGTTGCG)-3'	N = A, G, C, or T
cODN3(N)	5'-d(GCGTTGNATTGCG)-3'	N = A, G, C, or T
cODN4(N)	5'-d(GCGTTANGTTGCG)-3'	N = A, G, C, or T
cODN5(N)	5'-d(GCGTGANAGTGCG)-3'	N = A, G, C, or T
cODN6(N)	5'-d(GCGTCANACTGCG)-3'	N = A, G, C, or T
Probe _(JAK2)	5'-d(CCACAGA ^{3n7z} AACATACT)-3'	
Probe _(MTHFR)	5'-d(GAAATCG ^{3n7z} ACTCCCGC)-3'	
Probe _(DRD2)	5'-d(GGCTGTC ^{3n7z} AGGAGTGC)-3'	
JAK2(N)	5'-d(AGTATGINTCTGTGG)-3'	N = G or T
MTHFR(N)	5'-d(GCGGGAGNCGATTTC)-3'	N = C or T
DRD2(N)	5'-d(GCACTCCNGACAGCC)-3'	N = C or T

The thermal stabilities of the ODN duplexes containing ESF nucleoside ^{3n7z}A (**2**) were studied by measuring their melting temperatures. Specifically, ^{3n7z}A-containing single-stranded ODNs were hybridized with complementary ODNs, and the thermal stabilities of the resulting duplexes were assessed. As shown in Table 4, ^{3n7z}A-containing ODN duplexes exhibited high stability. The ^{3n7z}A-containing duplex ODN1(^{3n7z}A)/cODN1(T) presented a considerably higher melting temperature than other mismatched duplexes ODN1(^{3n7z}A)/cODN1(N) (N = A, G, or C) in sodium phosphate buffer (pH 7.0), suggesting that ^{3n7z}A (**2**) formed stable Watson-Crick base pairs, identified thymine when incorporated into ODN probes, and hybridized with target ODNs. Circular dichroism (CD) spectra displayed a negative peak at 250 nm and a positive peak at 280 nm for ^{3n7z}A-containing duplexes ODN1(^{3n7z}A)/cODN1(N) (N = A, G, C, or T) (Supplementary data, Fig. S4). These spectra also indicated that ^{3n7z}A (**2**) did not perturb the normal B-DNA structure.

Fluorescence spectra of ^{3n7z}A-containing duplexes comprising T/A or C/G base pairs flanking ^{3n7z}A (**2**) were obtained. An ODN probe containing the -T^{3n7z}AT- sequence (ODN1(^{3n7z}A)) was hybridized with complementary ODNs possessing matched and mismatched sequences, and its base-identification ability was assessed by fluorescence measurements (ODN1(^{3n7z}A)/cODN1(N), N = A, G, C, T). When the opposite base of the complementary strand was a perfectly matched thymine in the duplex, the fluorescence maximum was red-shifted to 416 nm (Fig. 4a and Table 4). When the opposite bases of the complementary strand were mismatched, strong broad emission bands appeared at shorter wavelengths (397, 398, and 410 nm for ODN1(^{3n7z}A)/cODN1(N) duplexes where N = C, G, or A, respectively). Interestingly, a significant thymine-selective wavelength shift was observed for ODN probes containing ^{3n7z}A (**2**) at C/G-rich sites (ODN2(^{3n7z}A)). When the opposite base of the complementary strand was the perfectly matched thymine (ODN2(^{3n7z}A)/cODN2(T)), the emission maximum was considerably red-shifted compared to other mismatched duplexes (ODN2(^{3n7z}A)/cODN2(N), N = C, G, or A), leading to a strong broad

Table 4. Thermal melting temperatures (T_m) and photophysical properties of oligonucleotides^a

ODNs	T_m (°C)	$\lambda_{\text{max}}^{\text{em}}$ (nm)	$\Phi_{\text{f}}^{\text{b}}$
ODN1(^{3n7z} A)	-	407	0.07
ODN1(^{3n7z} A)/cODN1(A)	48.1	410	0.07
/cODN1(G)	48.0	398	0.17
/cODN1(C)	49.4	397	0.22
/cODN1(T)	53.0	416	0.09
ODN1(A)/cODN1(T)	54.1	-	-
ODN2(^{3n7z} A)	-	395	0.16
ODN2(^{3n7z} A)/cODN2(A)	57.0	417	0.06
/cODN2(G)	57.8	398	0.05
/cODN2(C)	57.7	395	0.04
/cODN2(T)	62.3	428	0.20
ODN2(A)/cODN2(T)	63.3	-	-
ODN3(^{3n7z} A)	-	395	0.18
ODN3(^{3n7z} A)/cODN3(A)	51.9	410	0.09
/cODN3(G)	54.4	395	0.17
/cODN3(C)	53.2	395	0.13
/cODN3(T)	56.4	422	0.18
ODN3(A)/cODN3(T)	58.3	-	-
ODN4(^{3n7z} A)	-	401	0.12
ODN4(^{3n7z} A)/cODN4(A)	51.1	406	0.04
/cODN4(G)	51.6	398	0.02
/cODN4(C)	52.1	398	0.03
/cODN4(T)	57.0	421	0.12
ODN4(A)/cODN4(T)	60.1	-	-
ODN5(^{3n7z} A)	-	397	0.08
ODN5(^{3n7z} A)/cODN5(A)	53.7	407	0.06
/cODN5(G)	54.1	397	0.20
/cODN5(C)	55.3	397	0.20
/cODN5(T)	59.6	418	0.11
ODN5(A)/cODN5(T)	61.0	-	-
ODN6(^{3n7z} A)	-	406	0.02
ODN6(^{3n7z} A)/cODN6(A)	50.6	407	0.07
/cODN6(G)	52.0	398	0.23
/cODN6(C)	53.5	398	0.19
/cODN6(T)	57.1	418	0.14
ODN6(A)/cODN6(T)	60.1	-	-

^a ODNs (2.5 μM) were measured in 50 mM sodium phosphate and 0.1 M sodium chloride (pH 7.0) at room temperature

^b Fluorescence quantum yields were calculated according to Ref.10

emission band at 428 nm (Fig. 4b). The fluorescence emission of the mismatched duplexes was strongly quenched by the C/G base pairs flanking ^{3n7z}A (**2**),¹¹ resulting in thymine-selective fluorescence emission. The naphthalene moiety that was attached to 8-aza-3,7-dideazaadenine of ^{3n7z}A (**2**) at the C-3 position is extruded to the minor groove in a highly polar aqueous phase in matched duplexes because of thymine base pairing, explaining the thymine-selective red-shifted emission. In contrast, the naphthalene was located in a hydrophobic site inside the duplex in the absence of base-pairing (mismatched), causing ^{3n7z}A (**2**) to emit at a shorter wavelength. Moreover, strong fluorescence quenching was observed in the mismatched duplexes when the C/G base pairs flanked ^{3n7z}A (**2**) (ODN2(^{3n7z}A)), enhancing of the base-identification ability of ^{3n7z}A-containing ODN probes. Different bases were introduced on either side of the modified nucleoside to compare the properties of ^{3n7z}A (**2**) in various ODNs and investigated the quenching effect of the C/G base pairs flanking ^{3n7z}A (**2**). Significant changes in the emission wavelength and intensity revealed that ODN duplexes containing one C/G base pair flanking ^{3n7z}A (**2**) (ODN3(^{3n7z}A) and ODN4(^{3n7z}A)) identified the perfectly matched thymine in target ODNs (Fig. 4c-d). In particular, ODN4(^{3n7z}A)/cODN4 duplexes exhibited strong fluorescence quenching with high signal-to-noise (S/N) ratio, demonstrating that a C/G base pair flanking ^{3n7z}A (**2**) in the 3' to 5' direction significantly contributed to quenching in mismatched

duplexes. As shown in Fig. 4e-f, ODN duplexes containing the C/G base pairs separated by one A/T base pair from ^{3n7z}A (2) in 3'-to-5' and 5'-to-3' directions (ODN5(^{3n7z}A)/cODN5 and ODN6(^{3n7z}A)/cODN6) also clearly identified thymine and showed an emission wavelength shift without fluorescence quenching, indicating that only the C/G base pairs flanking ^{3n7z}A (2) acted as quenchers in the mismatched duplexes.

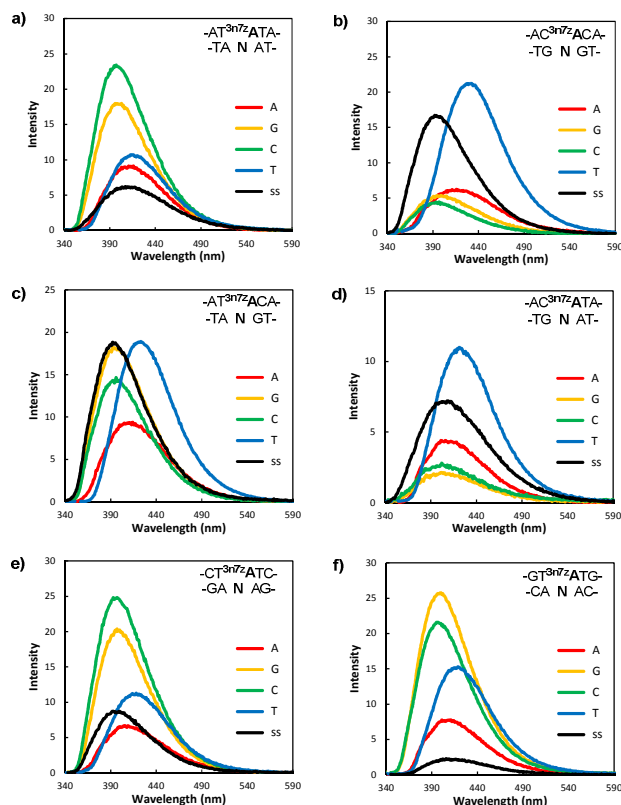


Figure 4. Fluorescence spectra of 2.5 μ M (a) ODN1(^{3n7z}A), (b) ODN2(^{3n7z}A), (c) ODN3(^{3n7z}A), (d) ODN4(^{3n7z}A), (e) ODN5(^{3n7z}A), and (f) ODN6(^{3n7z}A) hybridized with their complementary cODN1(N) - cODN6(N) (50 mM sodium phosphate, 0.1 M sodium chloride, pH 7.0, rt). "ss" denotes single-stranded ODN(^{3n7z}A). ODN and cODN concentrations both amounted to 2.5 μ M.

A clear change in emission observed in ^{3n7z}A -containing ODNs according to the type of the base in the complementary strand may prove very useful for SNP typing and gene sequence detection. Therefore, the performance of ^{3n7z}A -containing probes in SNP detection was assessed for T/G (T-allele/G-allele) and T/C (T-allele/C-allele) sequences, such as tyrosine kinase JAK2 (-TTT- (mutant)/-TGT- (wild type)),¹² human methylenetetrahydrofolate reductase MTHFR (-GTC- (mutant)/-GCC- (wild type)),¹³ and dopamine D2 receptor DRD2 (-CTG- (mutant)/-CCG- (wild type))¹⁴ (Table 3). The probes were added to each target sequence solutions, and these mixtures were incubated at room temperature for 1 min before fluorescence measurements. For the JAK2 sequence in which no C/G base pair flanked the target base in the duplex, strong fluorescence emission at approximately 400 nm was observed when mismatched guanine was opposite ^{3n7z}A (2) (Probe_(JAK2)/JAK2(G), wild type). In contrast, when the opposite base of the complementary strand was the perfectly matched thymine

(Probe_(JAK2)/JAK2(T), mutant), a strong emission was detected at 424 nm concomitant with a considerable red shift. No fluorescence quenching was observed when Probe_(JAK2) was present in the mismatched duplexes because no C/G base pairs flanked the target base in this SNP sequence. However, ODN probes containing ^{3n7z}A (2) identified thymine in target DNA by exhibiting a distinct emission wavelength change even for these sequences (Fig. 5, Table 5).

Next, the detection of MTHFR and DRD2, in which the C/G base pairs flanked the target base, was investigated. Probe_(MTHFR) and Probe_(DRD2) were hybridized with these target DNAs, and their corresponding fluorescence spectra were determined. Perfectly matched duplexes (mutant) exhibited strong fluorescence emission at a significantly red-shifted wavelength, whereas their mismatched counterparts (wild type) showed considerable fluorescence quenching (Fig. 5c, e). The fluorescence color change was readily observable by naked eye under illumination with 365 nm transilluminator (Fig 5d, f). These results indicate that when incorporated into ODNs, ESF nucleoside ^{3n7z}A (2) effectively detect thymine in target DNA by dramatically changing the emission wavelength and intensity, especially for SNP sequences containing the C/G base pairs flanking the target base.

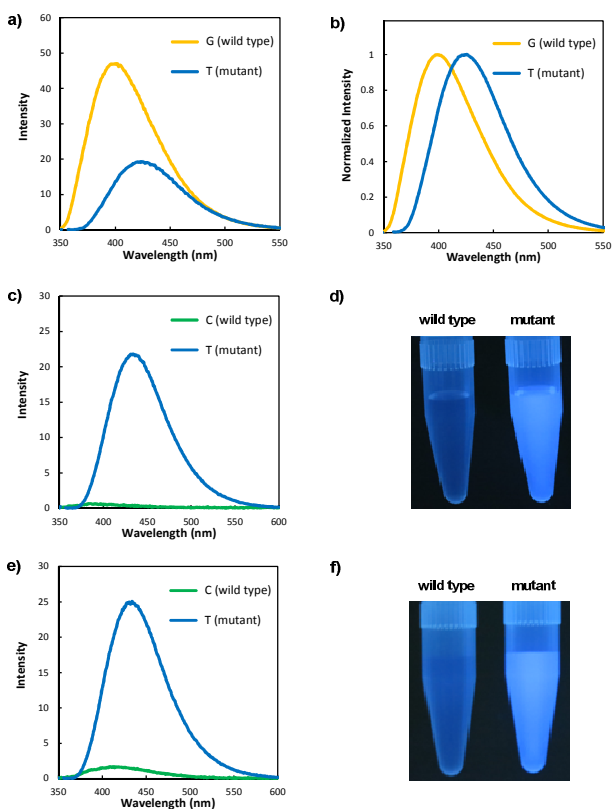


Figure 5. (a) Fluorescence and (b) normalized fluorescence spectra of Probe_(JAK2) (2.5 μ M) hybridized with JAK2(G) or JAK2(T) (2.5 μ M). (c) Fluorescence spectra of Probe_(MTHFR) (2.5 μ M) hybridized with MTHFR(C) or MTHFR(T) (2.5 μ M). (d) Fluorescence image of Probe_(MTHFR) hybridized with MTHFR(C) (left) or MTHFR(T) (right). (e) Fluorescence spectra of Probe_(DRD2) (2.5 μ M) hybridized with DRD2(C) or DRD2(T) (2.5 μ M). (f) Fluorescence image of Probe_(DRD2) hybridized with DRD2(C) (left) or DRD2(T) (right). Duplexes were measured in 50 mM sodium phosphate, and 0.1 M sodium chloride (pH 7.0) at room temperature. Sample solutions in (d) and (f) were irradiated with a 365 nm transilluminator.

Table 5. Thermal melting temperatures (T_m) and photophysical properties of 3n7z A-containing probe ODNs hybridized with their target sequences^a

ODNs	T_m (°C)	λ_{max}^{em} (nm)	Φ_f^b
Probe _{JAK2} /JAK2(G)	53.9	400	0.43
Probe _{JAK2} /JAK2(T)	54.8	424	0.18
Probe _{MTHFR} /MTHFR(C)	58.0	384	0.01
Probe _{MTHFR} /MTHFR(T)	61.9	434	0.22
Probe _{DRD2} /DRD2(C)	60.8	407	0.02
Probe _{DRD2} /DRD2(T)	63.5	434	0.25

^a Duplexes (2.5 μ M) were measured in 50 mM sodium phosphate and 0.1 M sodium chloride (pH 7.0) at room temperature
^b Fluorescence quantum yields were calculated according to Ref.10

Conclusions

8-Aza-3,7-dideaza-2'-deoxyadenosine **1** and its C3-naphthylethynylated derivative 3n7z A (**2**) comprising a 8-aza-3,7-dideazapurine (pyrazolo[4,3-c]pyridine) skeleton were successfully synthesized. Nucleoside 3n7z A (**2**) exhibited remarkable solvatochromic properties ($\Delta\lambda = 47$ nm) and environmentally sensitive ICT emission because of the electron transition of the coplanar conformer adopted by nucleobase and naphthalene moieties. Thermal melting data and CD spectra showed that ODN probes containing 3n7z A (**2**) only formed stable base pairs with thymine in DNA duplexes and maintained a stable B-DNA structure. Microenvironmental changes caused by the modifications of the opposite bases of 3n7z A (**2**) in the duplexes considerably shifted the emission wavelength. In particular, ODN probes containing 3n7z A (**2**) at the C/G-rich sites identified the perfectly matched thymine in target ODNs by significantly affecting the emission wavelength and intensity. Therefore, fluorescent DNA probes containing this base-modified ESF nucleoside may act as tools to discriminate full matches from mismatches and find application in gene detection, SNP typing, and molecular diagnostics.

Experimental section

General

¹H-NMR spectra (400 MHz) and ¹³C-NMR spectra (100 MHz) were measured on a JEOL JNM ECX-400 spectrometer. Coupling constant (J value) are reported in hertz. The chemical shifts are shown in ppm downfield from tetramethylsilane, using residual dimethyl sulfoxide (δ 2.50 in ¹H-NMR, δ 39.5 in ¹³C-NMR), chloroform (δ 7.26 in ¹H-NMR, δ 77.0 in ¹³C-NMR) and acetone (δ 2.05 in ¹H-NMR, δ 29.8 in ¹³C-NMR) as an internal standard. ESI-TOF masses were recorded on a JMS-T100LC "AccuTOF", Applied DATUM Solution Business Operations.

The reagents for DNA synthesis were purchased from Glen Research. Mass spectra of oligodeoxynucleotides were determined with a MALDI-TOF mass (Shimadzu AXIMA-LNR, positive mode) with 2',3',4'-trihydroxyacetophenone as a matrix. Calf intestinal alkaline phosphatase (Promega), *Crotalus adamanteus* venom phosphodiesterase I (USB), and *Penicillium citrinum* nuclease P1 (Yamasa Shoyu) were used for the enzymatic digestion of ODNs. All aqueous solutions utilized purified water (Millipore, Milli-Q sp UF).

Reversed-phase HPLC was performed on CHEMCOBOND 5-ODS-H columns (10 \times 150 mm, 4.6 \times 150 mm) with a JASCO Chromatograph, Model PU-2080, using a UV detector, Model UV-2075 plus at 260 nm.

Glycosylation of 4-chloro-1H-pyrazolo[4,3-c]pyridine (**3**) with 2-deoxy-3,5-di-O-(*p*-toluoyl)- α -D-ribofuranosyl chloride (**4**)

To a suspension of 4-chloro-1H-pyrazolo[4,3-c]pyridine **3** (810 mg, 5.3 mmol) in anhydrous acetonitrile (90 ml) was added NaH (60 %; 274 mg, 6.8 mmol), and the reaction mixture was stirred at 50 °C for 1 h. After cooling to room temperature, 2-deoxy-3,5-di-O-(*p*-toluoyl)- α -D-ribofuranosyl chloride **4** (2.15 g, 5.5 mmol) was added in small portions, and stirred at room temperature for 30 min. The mixture was filtered and the filtrate was concentrated in *vacuo*. The residue was purified by a silica gel column, eluted with CHCl₃/AcOEt (30:1-20:1), to give **5a** (1.20 g, 45 %) as a colorless solid from the first zone and to give **5b** (638 mg, 24 %) as a colorless solid from the second zone:

4-Chloro-1-(2-deoxy-3,5-di-O-(*p*-toluoyl)- β -D-ribofuranosyl)pyrazolo[4,3-c]pyridine (**5a**)

¹H-NMR (DMSO-*d*₆, 400 MHz) δ 2.38 (s, 3H), 2.41 (s, 3H), 2.79 (ddd, $J = 4.4, 6.4, 13.6$, 1H), 3.36 (m, 1H), 4.36 (m, 1H), 4.51 (m, 1H), 4.59 (m, 1H), 5.85 (m, 1H), 6.90 (m, 1H), 7.31 (m, 2H), 7.38 (m, 2H), 7.80 (m, 2H), 7.94-7.98 (complex, 3H), 8.23 (d, $J = 6.0$ Hz, 1H), 8.46 (s, 1H); ¹³C-NMR (DMSO-*d*₆, 100 MHz) δ 21.2, 21.2, 35.7, 63.8, 74.7, 81.7, 86.4, 105.4, 119.8, 126.5 (2C), 129.2 (2C), 129.2 (2C), 129.3 (2C), 129.5 (2C), 134.2, 143.5, 143.7, 143.8, 144.1, 144.4, 165.3 (2C); HRMS (ESI) m/z 528.1302 calcd for C₂₇H₂₄ClN₃O₅Na [M + Na]⁺, found 528.1325.

4-Chloro-2-(2-deoxy-3,5-di-O-(*p*-toluoyl)- β -D-ribofuranosyl)pyrazolo[4,3-c]pyridine (**5b**)

¹H-NMR (DMSO-*d*₆, 400 MHz) δ 2.36 (s, 3H), 2.41 (s, 3H), 2.90 (ddd, $J = 4.8, 7.2, 14.4$, 1H), 3.23 (m, 1H), 4.49 (m, 1H), 4.64 (m, 1H), 4.70 (m, 1H), 5.88 (m, 1H), 6.72 (m, 1H), 7.25 (m, 2H), 7.38 (m, 2H), 7.57 (d, $J = 6.4$ Hz, 1H), 7.80 (m, 2H), 7.95 (m, 2H), 8.02 (d, $J = 6.4$ Hz, 1H), 9.01 (s, 1H); ¹³C-NMR (DMSO-*d*₆, 100 MHz) δ 21.2, 21.2, 37.3, 63.8, 74.6, 82.7, 90.7, 111.4, 118.2, 126.3, 126.4, 126.5, 129.2 (2C), 129.2 (2C), 129.4 (2C), 129.5 (2C), 141.5, 143.8, 144.1, 145.0, 150.4, 165.3, 165.4; HRMS (ESI) m/z 528.1302 calcd for C₂₇H₂₄ClN₃O₅Na [M + Na]⁺, found 528.1326.

4-Chloro-1-(2-deoxy- β -D-ribofuranosyl)pyrazolo[4,3-c]pyridine (**6a**)

A suspension of **5a** (1.18 g, 2.3 mmol) in 0.5 M NaOMe/MeOH (50 ml) was stirred at room temperature for 30 min. After neutralization with dilute hydrochloric acid, the mixture was filtered, and the filtrate was concentrated in *vacuo*. The residue was purified by a silica gel column, eluted with CHCl₃/MeOH (20:1-15:1), to give **6a** (566 mg, 90 %) as a colorless solid: ¹H-NMR (DMSO-*d*₆, 400 MHz) δ 2.33 (ddd, $J = 4.8, 6.4, 13.2$ Hz, 1H), 2.87 (m, 1H), 3.34 (m, 1H), 3.50 (m, 1H), 3.85 (m, 1H), 4.47 (m, 1H), 4.75 (dd, $J = 5.2, 5.6$ Hz, 1H), 5.35 (d, $J = 4.0$ Hz, 1H), 6.64 (dd, $J = 6.0, 6.4$ Hz, 1H), 7.92 (d, $J = 6.0$ Hz, 1H), 8.22 (d, $J = 6.0$ Hz, 1H), 8.42 (s, 1H); ¹³C-NMR (DMSO-*d*₆, 100 MHz) δ 38.4, 62.1, 70.8, 86.4, 87.9, 105.5, 119.7, 133.7, 143.4, 143.6, 144.0; HRMS (ESI) m/z 292.0465 calcd for C₁₁H₁₂ClN₃O₃Na [M + Na]⁺, found 292.0468.

4-Chloro-2-(2-deoxy- β -D-ribofuranosyl)pyrazolo[4,3-c]pyridine (6b)

In the similar manner as described for **6a**, **5b** (824 mg, 1.6 mmol) was treated with 0.5 M NaOMe/MeOH (40 ml) to give **6b** (373 mg, 85 %) as a colorless solid: $^1\text{H-NMR}$ (DMSO- d_6 , 400 MHz) δ 2.44 (ddd, $J = 5.2, 6.8, 13.2$ Hz, 1H), 2.66 (m, 1H), 3.53 (m, 1H), 3.65 (m, 1H), 3.95 (m, 1H), 4.42 (m, 1H), 4.99 (dd, $J = 5.2, 5.6$ Hz, 1H), 5.36 (d, $J = 4.8$ Hz, 1H), 6.45 (dd, $J = 5.2, 6.4$ Hz, 1H), 7.61 (d, $J = 6.0$ Hz, 1H), 8.02 (d, $J = 6.0$ Hz, 1H), 9.02 (s, 1H); $^{13}\text{C-NMR}$ (DMSO- d_6 , 100 MHz) δ 40.7, 61.4, 70.0, 88.6, 91.1, 111.4, 118.1, 124.9, 141.3, 144.8, 150.1; HRMS (ESI) m/z 292.0465 calcd for $\text{C}_{11}\text{H}_{12}\text{ClN}_3\text{O}_3\text{Na}$ [M + Na] $^+$, found 292.0471.

4-Amino-1-(2-deoxy- β -D-ribofuranosyl)pyrazolo[4,3-c]pyridine (1)

A solution of **6a** (800 mg, 3.0 mmol) in anhydrous hydrazine (8 ml) was stirred at 90 °C for 2 h. The reaction mixture was concentrated *in vacuo*, and the residue was co-evaporated with ethanol removed hydrazine. The residue was dissolved in ethanol (50 ml) in the presence of Raney-Nickel, and was stirred for 2 h under reflux. The reaction mixture was filtered through Celite while hot and the catalyst was washed with hot ethanol, and the filtrate was concentrated *in vacuo*. The residue was purified by a silica gel column, eluted with $\text{CHCl}_3/\text{MeOH}/\text{NH}_4\text{OH}$ (90:9:1), to give **1** (400 mg, 54 %) as a colorless solid: $^1\text{H-NMR}$ (DMSO- d_6 , 400 MHz) δ 2.24 (ddd, $J = 4.0, 6.8, 13.2$ Hz, 1H), 2.83 (m, 1H), 3.33 (m, 1H), 3.48 (m, 1H), 3.80 (m, 1H), 4.42 (m, 1H), 4.74 (m, 1H), 5.27 (d, $J = 4.8$ Hz, 1H), 6.40 (m, 1H), 6.74 (br, 2H), 6.83 (d, $J = 6.4$ Hz, 1H), 7.68 (d, $J = 6.4$ Hz, 1H), 8.21 (s, 1H); $^{13}\text{C-NMR}$ (DMSO- d_6 , 100 MHz) δ 38.3, 62.4, 71.0, 85.6, 87.5, 94.6, 108.1, 133.8, 144.0, 144.4, 154.0; HRMS (ESI) m/z 273.0964 calcd for $\text{C}_{11}\text{H}_{14}\text{N}_4\text{O}_3\text{Na}$ [M + Na] $^+$, found 273.0958.

4-Amino-1-(2-deoxy-3,5-di-*O*-tert-butylidimethylsilyl- β -D-ribofuranosyl)pyrazolo[4,3-c]pyridine (7)

A mixture of **1** (170 mg, 0.68 mmol), *tert*-butylidimethylsilyl chloride (512 mg, 3.4 mmol), and imidazole (462 mg, 6.8 mmol) in dry DMF (5 ml) was stirred at room temperature for overnight. The reaction solution was concentrated *in vacuo*, and the residue was dissolved in ethyl acetate, which was washed with saturated NH_4Cl , followed by brine. The separated organic layer was dried with anhydrous Na_2SO_4 , filtered and concentrated. The residue was purified by a silica gel column, eluted with $\text{CHCl}_3/\text{MeOH}$ (50:1), to give **7** (245 mg, 75 %) as a colorless oil: $^1\text{H-NMR}$ (CDCl_3 , 400 MHz) δ -0.02 (s, 3H), -0.01 (s, 3H), 0.13 (s, 6H), 0.86 (s, 9H), 0.93 (s, 9H), 2.29 (ddd, $J = 3.2, 6.4, 13.2$ Hz, 1H), 3.05 (m, 1H), 3.65 (complex, 2H), 3.99 (m, 1H), 4.66 (m, 1H), 5.08 (br, 2H), 6.38 (m, 1H), 6.91 (d, $J = 6.4$ Hz, 1H), 7.85 (d, $J = 6.4$ Hz, 1H), 7.93 (s, 1H); $^{13}\text{C-NMR}$ (CDCl_3 , 100 MHz) δ -5.5 (2C), -4.7 (2C), 18.0, 18.4, 25.8 (3C), 25.9 (3C), 38.7, 63.5, 72.8, 86.9, 87.9, 97.0, 109.1, 132.3, 143.5, 144.9, 152.8; HRMS (ESI) m/z 501.2693 calcd for $\text{C}_{23}\text{H}_{42}\text{N}_4\text{O}_3\text{Si}_2\text{Na}$ [M + Na] $^+$, found 501.2713.

4-Amino-1-(2-deoxy-3,5-di-*O*-tert-butylidimethylsilyl- β -D-ribofuranosyl)-7-iodopyrazolo[4,3-c]pyridine (8)

A mixture of **7** (230 mg, 0.48 mmol) and *N*-iodosuccinimide (216 mg, 0.96 mmol) in dry DMF (6 ml) was stirred at room temperature for overnight. The reaction solution was concentrated *in vacuo*, and the residue was dissolved in ethyl acetate, which was washed with saturated $\text{Na}_2\text{S}_2\text{O}_3$, followed by brine. The separated organic layer

was dried with anhydrous Na_2SO_4 , filtered and concentrated. The residue was purified by a silica gel column, eluted with $\text{CHCl}_3/\text{MeOH}$ (100:1), to give **8** (272 mg, 96 %) as a colorless oil: $^1\text{H-NMR}$ (CDCl_3 , 400 MHz) δ -0.05 (s, 3H), -0.02 (s, 3H), 0.14 (s, 6H), 0.85 (s, 9H), 0.94 (s, 9H), 2.32 (ddd, $J = 4.0, 6.4, 13.2$ Hz, 1H), 3.14 (ddd, $J = 6.0, 6.0, 13.2$ Hz, 1H), 3.58-3.66 (complex, 2H), 4.00 (m, 1H), 4.69 (m, 1H), 5.09 (br, 2H), 7.41 (dd, $J = 6.0, 6.4$ Hz, 1H), 7.84 (s, 1H), 8.13 (s, 1H); $^{13}\text{C-NMR}$ (CDCl_3 , 100 MHz) δ -5.4 (2C), -4.7, -4.6, 18.0, 18.3, 25.8 (3C), 25.9 (3C), 38.5, 57.5, 63.6, 72.8, 84.8, 87.6, 111.3, 132.3, 143.8, 152.5, 152.8; HRMS (ESI) m/z 627.1660 calcd for $\text{C}_{23}\text{H}_{41}\text{I}\text{N}_4\text{O}_3\text{Si}_2\text{Na}$ [M + Na] $^+$, found 627.1681.

4-Amino-1-(2-deoxy- β -D-ribofuranosyl)-7-iodopyrazolo[4,3-c]pyridine (9)

A THF solution of TBAF (1 M, 0.90 ml, 0.90 mmol) was added to a solution of **8** (260 mg, 0.43 mmol) in THF (10 ml) at room temperature and the reaction mixture was stirred for 1 h. After addition of AcOH (51 μl , 0.90 mmol), the reaction solution was concentrated *in vacuo*, and the residue was purified by a silica gel column, eluted with $\text{CHCl}_3/\text{MeOH}$ (12:1-8:1), to give **9** (136 mg, 84 %) as a colorless solid: $^1\text{H-NMR}$ (DMSO- d_6 , 400 MHz) δ 2.29 (ddd, $J = 4.4, 6.0, 13.2$ Hz, 1H), 2.99 (ddd, $J = 6.0, 6.0, 13.2$ Hz, 1H), 3.27 (m, 1H), 3.44 (m, 1H), 3.80 (m, 1H), 4.44 (m, 1H), 4.68 (dd, $J = 5.6, 5.6$ Hz, 1H), 5.25 (d, $J = 4.4$ Hz, 1H), 6.96 (br, 2H), 7.27 (dd, $J = 6.0, 6.0$ Hz, 1H), 7.96 (s, 1H), 8.23 (s, 1H); $^{13}\text{C-NMR}$ (DMSO- d_6 , 100 MHz) δ 38.1, 55.4, 62.4, 71.1, 84.2, 87.6, 110.6, 133.9, 143.0, 152.7, 154.0; HRMS (ESI) m/z 398.9930 calcd for $\text{C}_{11}\text{H}_{13}\text{I}\text{N}_4\text{O}_3\text{Na}$ [M + Na] $^+$, found 398.9940.

4-Amino-1-(2-deoxy- β -D-ribofuranosyl)-7-(1-naphthylethynyl)pyrazolo[4,3-c]pyridine (2: ^{3n7z}A)

A mixture of **9** (61.1 mg, 0.16 mmol), $\text{Pd}(\text{PPh}_3)_4$ (9.4 mg, 0.81×10^{-2} mmol), CuI (1.5 mg, 0.79×10^{-2} mmol) and 1-ethynyl naphthalene (30.4 mg, 0.20 mmol) in dry DMF (5 ml) and Et_3N (0.3 ml) was stirred at 60 °C under argon atmosphere for 1 h. After cooling to room temperature, the reaction mixture was concentrated *in vacuo*. The residue was purified by silica gel column eluted with $\text{CHCl}_3/\text{MeOH}$ (15:1-10:1), to give **2** (62.0 mg, 95 %) as a pale yellow solid: $^1\text{H-NMR}$ (DMSO- d_6 , 400 MHz) δ 2.33 (ddd, $J = 4.0, 6.8, 13.2$ Hz, 1H), 3.01 (m, 1H), 3.38 (m, 1H), 3.52 (m, 1H), 3.91 (m, 1H), 4.49 (m, 1H), 4.75 (m, 1H), 5.29 (d, $J = 4.4$ Hz, 1H), 7.42 (m, 1H), 7.43 (br, 2H), 7.54-7.72 (complex, 3H), 7.85-8.02 (complex, 3H), 8.18 (s, 1H), 8.39 (s, 1H), 8.47 (m, 1H); $^{13}\text{C-NMR}$ (DMSO- d_6 , 100 MHz) δ 38.2, 62.4, 71.1, 85.5, 87.8, 89.9, 90.9, 91.5, 107.6, 120.5, 125.6, 125.8, 126.7, 127.4, 128.4, 128.4, 129.9, 132.0, 132.9, 134.6, 142.2, 150.0, 154.2; HRMS (ESI) m/z 423.1433 calcd for $\text{C}_{23}\text{H}_{20}\text{N}_4\text{O}_3\text{Na}$ [M + Na] $^+$, found 423.1460.

1-(2-Deoxy- β -D-ribofuranosyl)-4-(*N,N*-di-*n*-butylformamidino)amino-7-(1-naphthylethynyl)pyrazolo[4,3-c]pyridine (10)

To a solution of **2** (40.0 mg, 0.10 mmol) in DMF (2 ml) was added *N,N*-di-*n*-butylformamide dimethyl acetal (72 μl , 0.30 mmol), and the reaction mixture was stirred at 80 °C for 2 h. After cooling to room temperature, the reaction mixture was concentrated *in vacuo*. The residue was purified by silica gel column eluted with $\text{CHCl}_3/\text{MeOH}$ (100:1-50:1), to give **10** (42.0 mg, 78 %) as a pale

yellow oil: $^1\text{H-NMR}$ (DMSO- d_6 , 400 MHz) δ 0.95 (m, 6H), 1.34 (m, 4H), 1.62 (m, 4H), 2.36 (ddd, $J = 4.0, 6.8, 13.2$ Hz, 1H), 3.04 (m, 1H), 3.37 (m, 1H), 3.44-3.55 (complex, 3H), 3.62 (m, 2H), 3.92 (m, 1H), 4.51 (m, 1H), 4.75 (m, 1H), 5.30 (d, $J = 4.4$ Hz, 1H), 7.44 (m, 1H), 7.56-7.75 (complex, 3H), 7.91-8.03 (complex, 3H), 8.25 (s, 1H), 8.38 (s, 1H), 8.50 (m, 1H), 8.85 (s, 1H); $^{13}\text{C-NMR}$ (DMSO- d_6 , 100 MHz) δ 13.6, 13.7, 19.2, 19.6, 28.7, 30.6, 38.2, 44.5, 50.9, 62.5, 71.1, 85.5, 87.9, 89.5, 93.0, 95.2, 115.2, 120.1, 125.7, 125.8, 126.8, 127.5, 128.4, 128.9, 130.4, 132.0, 132.9, 135.2, 142.5, 149.1, 156.3, 157.2; HRMS (ESI) m/z 562.2794 calcd for $\text{C}_{32}\text{H}_{37}\text{N}_5\text{O}_3\text{Na}$ [$\text{M} + \text{Na}$] $^+$, found 562.2776.

1-[2-Deoxy-5-O-(4,4'-dimethoxytrityl)- β -D-ribofuranosyl]-4-(*N,N*-di-*n*-butylformamidino)amino-7-(1-naphthylethynyl)pyrazolo[4,3-*c*]pyridine (11)

A mixture of **10** (42.0 mg, 7.8×10^{-2} mmol) and 4,4'-dimethoxytrityl chloride (31.6 mg, 9.3×10^{-2} mmol) in anhydrous pyridine (2 ml) was stirred at room temperature for 2 h. After reaction was complete, quenched by addition of methanol, and the solvent was concentrated in *vacuo*. The residue was partitioned between ethyl acetate and saturated NaHCO_3 , and the separated organic layer was washed with brine. The organic layer was dried with anhydrous Na_2SO_4 , filtered and concentrated. The residue was purified by silica gel column eluted with $\text{CHCl}_3/\text{MeOH}$ (200:1-100:1), to give **11** (64.2 mg, 98 %) as a pale yellow solid: $^1\text{H-NMR}$ (Acetone- d_6 , 400 MHz) δ 1.00 (m, 6H), 1.43 (m, 4H), 1.73 (m, 4H), 2.51 (m, 1H), 3.16 (m, 1H), 3.20-3.28 (complex, 2H), 3.53 (t, $J = 7.2$ Hz, 2H), 3.68-3.72 (complex, 8H), 4.21 (m, 1H), 4.46 (d, $J = 4.8$ Hz, 1H), 4.86 (m, 1H), 6.70 (m, 4H), 7.09-7.41 (complex, 9H), 7.54 (dd, $J = 4.0, 6.8$ Hz, 1H), 7.56-7.73 (complex, 3H), 7.97-8.01 (complex, 3H), 8.16 (s, 1H), 8.42 (s, 1H), 8.74 (m, 1H), 8.92 (s, 1H); $^{13}\text{C-NMR}$ (Acetone- d_6 , 100 MHz) δ 14.0, 14.2, 20.4, 20.8, 30.0, 31.9, 39.7, 45.9, 52.4, 55.4 (2C), 65.6, 72.7, 86.5, 86.9, 87.1, 90.7, 93.7, 97.2, 113.7 (4C), 117.0, 122.0, 126.4, 127.2, 127.2, 127.5, 128.1, 128.3 (2C), 129.0 (2C), 129.2, 129.5, 130.8 (2C), 131.0 (2C), 131.3, 133.7, 134.3, 135.9, 136.9, 137.0, 143.9, 146.4, 150.0, 157.1, 158.5, 159.3, 159.4; HRMS (ESI) m/z 864.4101 calcd for $\text{C}_{53}\text{H}_{55}\text{N}_5\text{O}_5\text{Na}$ [$\text{M} + \text{Na}$] $^+$, found 864.4109.

1-[2-Deoxy-5-O-(4,4'-dimethoxytrityl)- β -D-ribofuranosyl]-4-(*N,N*-di-*n*-butylformamidino)amino-7-(1-naphthylethynyl)pyrazolo[4,3-*c*]pyridine 2-cyanoethyl-*N,N'*-diisopropylphosphoramidite (12)

To a solution of **11** (64.2 mg, 7.8×10^{-2} mmol) in anhydrous acetonitrile (1 ml) was added 2-cyanoethyl-diisopropylchlorophosphoramidite (100 μl) in the presence of Et_3N (0.5 ml), and stirred at room temperature under an argon atmosphere for 30 min. After completion of the reaction, the solution was diluted with ethyl acetate, washed with saturated NaHCO_3 and brine. The combined organic layer was dried with anhydrous Na_2SO_4 , filtered and concentrated. The residue was incorporated into oligonucleotides without further purification.

Oligodeoxynucleotide synthesis and characterization

Oligodeoxynucleotide (ODN) sequences were synthesized by a conventional phosphoramidite method by using an Applied Biosystems 3400 DNA/RNA synthesizer. ODNs were purified by reverse phase HPLC on a 5-ODS-H column (10 \times 150 nm, elution

with 50 mM ammonium formate (AF) buffer, pH 7.0, linear gradient over 45 min from 3 % to 20 % acetonitrile at a flow rate 2.0 ml/min). ODNs containing modified nucleotides were fully digested with calf intestine alkaline phosphatase (50 U/ml), and P1 nuclease (50 U/ml) at 37 $^\circ\text{C}$ for 12 h. Digested solutions were analyzed by HPLC on a CHEMCOBOND 5-ODS-H column (4.6 \times 150 nm, elution with a solvent mixture of 50 mM AF buffer, pH 7.0, flow rate 1.0 ml/min). The concentration of ODNs was determined by comparing peak areas with a standard solution containing dA, dG, dC, and dT at a concentration of 0.1 mM. Mass spectra of ODNs purified by HPLC were determined with a MALDI-TOF mass spectrometer.

Electrochemistry measurements

Electrochemistry measurements were performed at 25 $^\circ\text{C}$, using a BAS 100 W electrochemical analyzer in dehydrated acetonitrile containing 0.10 M TBAPF₆ (tetra-*n*-butylammonium hexafluorophosphate) as a supporting electrolyte. A conventional three-electrode cell was used with a platinum working electrode and a platinum wire as a counter electrode. The measured potentials were recorded with respect to the Ag/AgNO_3 (1.0×10^{-2} M) as a reference electrode. The potential values obtained vs Ag/AgNO_3 were converted vs saturated calomel electrode (SCE) using ferrocene.

UV-vis absorption and fluorescence measurements

Absorption spectra were obtained using a Shimadzu UV-2550 spectrophotometer at room temperature using 1 cm path length cell. Fluorescence spectra were obtained with a Shimadzu RF-5300PC spectrofluorophotometer at 25 $^\circ\text{C}$ using 1 cm path length cell. The excitation and emission bandwidths were 1.5 nm. The fluorescence quantum yields (Φ_f) were determined using 9,10-diphenylanthracene as a reference with the known Φ_f (0.95) in ethanol.¹⁰

Melting temperature (T_m) measurements

All T_m s of the ODNs (2.5 μM , final concentration) were measured in 50 mM sodium phosphate buffers (pH 7.0) containing 100 mM sodium chloride. Absorbance vs temperature profiles were measured at 260 nm using a Shimadzu UV-2550 spectrophotometer equipped with a Peltier temperature controller using 1 cm path length cell. The absorbance of the samples was monitored at 260 nm from 4 to 90 $^\circ\text{C}$ with a heating rate of 1 $^\circ\text{C}/\text{min}$. From these profiles, first derivatives were calculated to determine T_m values.

Circular dichroism (CD) measurements

CD spectra were recorded with a JASCO J-805 CD spectrophotometer. CD spectra of oligonucleotides solutions (2.5 μM ODNs in 50 mM sodium phosphate buffers (pH 7.0) containing 100 mM sodium chloride at 20 $^\circ\text{C}$) were measured using 2 mm path length cell.

Acknowledgements

This work was supported by a Grant-in-Aid for Scientific Research of MEXT, Japanese Government. A.S. thanks JSPS

Research Fellowships for Young Scientists. The authors thank Professor Isao Saito for helpful discussion.

Notes and references

- (a) L. D. Lavis and R. T. Raines, *ACS Chem. Biol.* 2008, **3**, 142-155; (b) R. W. Sinkeldam, N. J. Greco and Y. Tor, *Chem. Rev.*, 2010, **110**, 2579-2619; (c) N. Dai and E. T. Kool, *Chem. Soc. Rev.* 2011, **40**, 5756-5770.
- (a) A. Takahashi, Y. Zhang, V. E. Centonze and B. Herman, *BioTechniques*, 2001, **30**, 804-812; (b) T. Xia, *Curr. Opin. Chem. Biol.*, 2008, **12**, 604-611.
- (a) B. E. Cohen, T. B. McAnaney, E. S. Park, Y. N. Jan, S. G. Boxer and L. Y. Jan, *Science*, 2002, **296**, 1700-1703; (b) H. S. Lee, J. Guo, E. A. Lemke, R. D. Dimla and P. G. Schultz, *J. Am. Chem. Soc.*, 2009, **131**, 12921-12923.
- (a) M. J. Rist and J. P. Marino, *Curr. Org. Chem.*, 2002, **6**, 775-793; (b) M. Rist, N. Amann and H.-A. Wagenknecht, *Eur. J. Org. Chem.*, 2003, 2498-2504; (c) G. T. Hwang, Y. J. Seo and B. H. Kim, *J. Am. Chem. Soc.*, 2004, **126**, 6528-6529; (d) M. V. Skorobogatyi, A. D. Malakhov, A. A. Pchelintseva, A. A. Turban, S. L. Bondarev and V. A. Korshun, *ChemBioChem*, 2006, **7**, 810-816; (e) C. Grünwald, T. Kwon, N. Piton, U. Förster, J. Wachtveitl and J. W. Engels, *Bioorg. Med. Chem.*, 2008, **16**, 19-26; (f) A. A. Tanpure and S. G. Srivatsan, *Chem. Eur. J.*, 2011, **17**, 12820-12827; (g) M. G. Pawar and S. G. Srivatsan, *Org. Lett.*, 2011, **13**, 1114-1117; (h) R. W. Sinkeldam, A. J. Wheat, H. Boyaci and Y. Tor, *ChemPhysChem*, 2011, **12**, 567-570; (i) R. W. Sinkeldam, P. M. D. Uchenik and Y. Tor, *ChemPhysChem*, 2011, **12**, 2260-2265; (j) J. Riedl, R. Pohl, L. Rulísek and M. Hocek, *J. Org. Chem.*, 2012, **77**, 1026-1044; (k) A. A. Tanpure and S. G. Srivatsan, *ChemBioChem*, 2012, **13**, 2392-2399; (l) J. Riedl, P. Ménová, R. Pohl, P. Orság, M. Fojta and M. Hocek, *J. Org. Chem.*, 2012, **77**, 8287-8293.
- (a) Y. Saito, A. Suzuki, S. Ishioroshi and I. Saito, *Tetrahedron Lett.*, 2010, **51**, 2606-2609; (b) K. Matsumoto, N. Takahashi, A. Suzuki, T. Morii, Y. Saito and I. Saito, *Bioorg. Med. Chem. Lett.*, 2011, **21**, 1275-1278; (c) A. Suzuki, N. Takahashi, Y. Okada, I. Saito, N. Nemoto and Y. Saito, *Bioorg. Med. Chem. Lett.*, 2013, **23**, 886-892.
- (a) Y. Saito, A. Suzuki, Y. Okada, Y. Yamasaka, N. Nemoto and I. Saito, *Chem. Commun.*, 2013, **49**, 5684-5686; (b) A. Suzuki, N. Nemoto, I. Saito and Y. Saito, *Org. Biomol. Chem.*, 2014, **12**, 660-666; (c) A. Suzuki, T. Yanaba, I. Saito and Y. Saito, *ChemBioChem*, 2014, **15**, 1638-1644; (d) Y. Saito, A. Suzuki, T. Yamauchi and I. Saito, *Tetrahedron Lett.*, In press. DOI: 10.1016/j.tetlet.2014.10.116
- F. Seela and M. Zulauf, *J. Chem. Soc. Perkin Trans. 1*, 1998, 3233-3239.
- J. He and F. Seela, *Org. Biomol. Chem.*, 2003, **1**, 1873-1883.
- K. Sonogashira, Y. Tohda and N. Hagihara, *Tetrahedron Lett.*, 1975, **16**, 4467-4469.
- J. V. Morris, M. A. Mahaney and J. R. Huber, *J. Phys. Chem.*, 1976, **80**, 969-974.
- (a) Y. Saito, Y. Miyauchi, A. Okamoto and I. Saito, *Tetrahedron Lett.*, 2004, **45**, 7827-7831; (b) Y. Saito, E. Mizuno, S. S. Bag and I. Saito, *Chem. Commun.*, 2007, 4492-4494.
- (a) R. Kralovics, F. Passamonti, A. S. Buser, S.-S. Teo, R. Tiedt, J. R. Passweg, A. Tichelli, M. Cazzola and R. C. Skoda, *N. Engl. J. Med.*, 2005, **352**, 1779-1790; (b) E. J. Baxter, L. M. Scott, P. J. Campbell, C. East, N. Fourouclas, S. Swanton, G. S. Vassiliou, A. J. Bench, E. M. Boyd, N. Curtin, M. A. Scott, W. N. Erber and A. R. Green, *Lancet*, 2005, **365**, 1054-1061.
- (a) P. Frosst, H. J. Blom, R. Milos, P. Goyette, C. A. Sheppard, R. G. Matthews, G. J. H. Boers, M. den Heijer, L. A. J. Kluijtmans, L. P. van den Heuve and R. Rozen, *Nat. Genet.*, 1995, **10**, 111-113; (b) R. Castro, I. Rivera, P. Ravasco, M. E. Camilo, C. Jakobs, H. J. Blom and I. T. de Almeida, *J. Med. Genet.*, 2004, **41**, 454-458.
- (a) J. Duan, M. S. Wainwright, J. M. Comeron, N. Saitou, A. R. Sanders, J. Gelernter and P. V. Gejman, *Hum. Mol. Genet.*, 2003, **12**, 205-216; (b) S. Markett, C. Montag, C. Diekmann and M. Reuter, *Neurosci. Lett.*, 2014, **566**, 216-220.